

Microstructural evolution during sintering of CoO doped SnO₂ ceramics

J.A. Varela^{a,*}, J.A. Cerri^b, E.R. Leite^b, E. Longo^b, M. Shamsuzzoha^c, R.C. Bradt^c

^a*Instituto de Química, UNESP, Caixa Postal 355, 14800 Araraquara, SP, Brazil*

^b*Departamento de Química, UFSCar, Caixa Postal 676, 13560 São Carlos, SP, Brazil*

^c*Department of Metallurgical and Materials Engineering, University of Alabama, Tuscaloosa, AL, USA*

Received 11 September 1997; accepted 5 February 1998

Abstract

Addition of 0.5 mol% of CoO into SnO₂ promotes densification of this oxide to 99% of the theoretical density during sintering. TEM in this system reveals that after sintering at 1210°C a secondary phase of Co₂SnO₄ is precipitated at the SnO₂ grain boundaries during cooling. This phase is formed by diffusion of Co ions from the bulk to the grain boundary during sintering leaving needle-like defects at the grain bulk. The high resolution TEM micrograph of this system sintered at 1210°C and 1400°C showed an amorphous grain boundary region low in cobalt, indicating that the Co₂SnO₄ phase is precipitated from this region. © 1999 Elsevier Science Limited and Techna S.r.l. All rights reserved

1. Introduction

SnO₂ ceramics are n-type semiconductors that have many uses such as gas sensors, electrodes for electric glass melting furnaces, electrochromic devices, crystal displays, photodetectors, solar cells and protective coatings [1–3]. However the use of tin oxide ceramics is limited by the low densification during sintering due to the dominance of non-densifying mechanisms for mass transport such as surface diffusion or evaporation condensation [4]. These mechanisms promote grain coarsening of SnO₂ leading to low densification of this ceramics [5].

Several processes and sintering aids have been used to improve the densification of SnO₂ ceramics by forming lattice solid solution or liquid phase. For example, the addition of 2 mol% of CuO promotes a significative densification of SnO₂ due to the formation of a non-reactive liquid which is responsible for the rearrangement during the initial stage of sintering and for the formation of lattice defects in SnO₂ promoting an increase of diffusion through the SnO₂ lattice [6]. Zuca et al. [7] observed that SnO₂ densifies up to 94% of theoretical density when 2 mol% of Sb₂O₃ and 1 mol%

of CuO are used as additives. Park et al. [8] have obtained 97% of theoretical density of SnO₂ (without additives) by using hot isostatic pressing (150 MPa) at 1400°C during 12 h. They considered that the control of SnO₂ evaporation is fundamental to obtain high density in the polycrystalline SnO₂ ceramic during sintering.

The benefits of CoO to the sintering of SnO₂ was recently reported in the literature [9]. Densities above 99% of the theoretical density were obtained during sintering of CoO doped SnO₂ ceramics. The absence of experimental evidence for a eutectic liquid suggests that the densification observed for this system is not associated with liquid-phase sintering. Thus the sintering of CoO doped SnO₂ (up to 2.0 mol%) seems to be controlled by solid state diffusion. CoO in solutions within the SnO₂ structures acts as an acceptor leading to creation of additional oxygen vacancies in the SnO₂, increasing the densification rate of this oxide.

The segregation of MnO₂ on the surface of SnO₂ grains during sintering has been discussed by Gouvea et al. [10]. CoO like MnO₂ may segregate at the SnO₂ grain boundaries and create a large oxygen vacancy concentration there. The purpose of this study is to characterize by TEM, the grain boundary interface of CoO doped SnO₂ aiming to identify the grain boundary structure as well as possible secondary phase precipitation after sintering of CoO doped SnO₂.

* Corresponding author.

2. Experimental procedures

The characteristics of the oxides used in this study are described in Table 1. A study using a X-ray fluorescence (Model SRS 3000, Siemens, Karlsruhe, Germany) and IC Plasma revealed that the SnO_2 powder contains minor amounts of Pb (0.01%), Fe (<0.01%), Ge (<0.005%), and Cu (<0.005%) as major impurities. Doping of SnO_2 with 0.5 mol% of CoO was performed by mechanical mixing in isopropyl alcohol for 4 h, using polypropylene jars with yttrium stabilized zirconia balls to aid the mixing process. After drying, the powders were granulated and the pellets were isostatically pressed at 210 MPa, to a green density of $3.96 \pm 0.09 \text{ g/cm}^3$. The samples were sintered in a dilatometer (Model 402E NETZSCH Gerätebau, Selb, Germany) to 1400°C using a constant heating rate of 10°C/min .

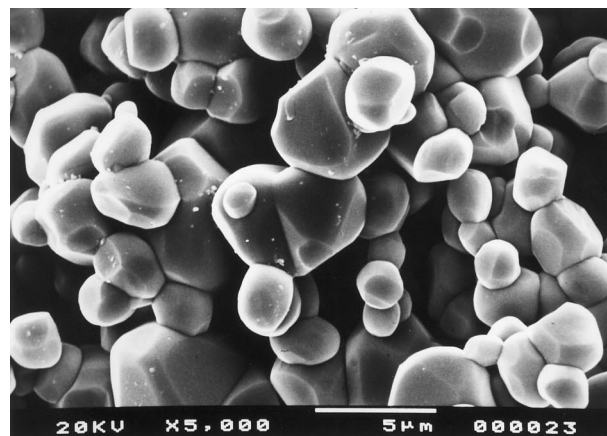
The microstructure of sintered pellets was characterized by scanning electron microscopy (SEM) and by transmission electron microscopy (TEM). For thin-foil preparation, cylindrical specimens of 3 mm diameter were cut by an ultrasonic disc cutter. These cylinders were then ground gently with a 600 grade silicon carbide paper to about $200 \mu\text{m}$ and then dimpled by mechanical polishing. These discs were then ion-mill thinned to a thickness of less than 100 nm to allow electron beam transmission. The thin foils thus prepared, were examined with a 200 keV TEM (Hitachi H-8000) equipped with EDS facilities to determine elemental composition of the specimens. High resolution electron microscopy (HREM) was performed with a JEM 4000 EX microscope operated at 400 keV. The high resolution electron micrographs were recorded near optimum defocus at a typical magnification of about 500,000. Secondary phase was determined by the EDS stage attached to the TEM and by electron diffraction. Sintering densities was measured using the Archimedes method.

3. Results and discussion

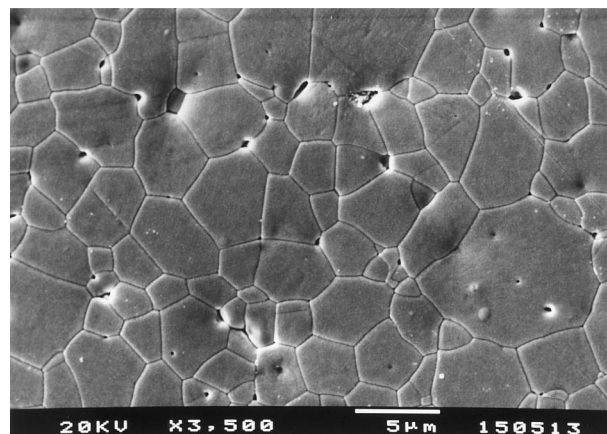
Fig. 1 shows the microstructures of the undoped SnO_2 and of the SnO_2 with a 0.5 mol% CoO addition sintered at 1400°C and observed in the SEM. As evident in these microstructures, the sintering of the undoped SnO_2 sample lead to grain coarsening without densification. The addition of 0.5 mol% of CoO to the SnO_2

lead to densification during sintering to higher than 99% of theoretical density.

To verify this drastic modification of the sintered SnO_2 structure, a high resolution transmission electron microscopy study was conducted in these samples considering two sintering temperatures, 1210°C and 1400°C (Fig. 2). An amorphous-like phase is observed in both micrograph at the grain boundary, indicating either a liquid phase or a region with a high defect density, probably with oxygen vacancies. The presence of a liquid phase is considered less probable since microanalysis of this region did not identify any Co. Thus this region may have a high concentration of oxygen vacancies due to segregation of Co^{+2} substituting Sn^{+4} ions. As observed in the micrograph of Fig. 2a there are many defects within the bulk of the SnO_2 grains probably related to defect cluster formation. These defects can be better identified in the micrograph of Fig. 3 where a large concentration of needle like defects are observed within the grain bulk of CoO doped SnO_2 sintered at 1210°C . These kind of defects appears to be



(a)



(b)

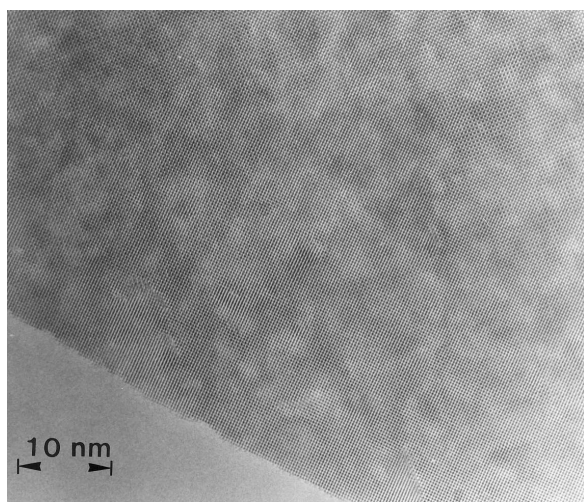
Fig. 1. SEM micrograph of SnO_2 pellet sintered at 1400°C during 1 h: (a) undoped; and (b) 0.5 mol% CoO doped.

Table 1
Chemical and physical characteristics of oxides

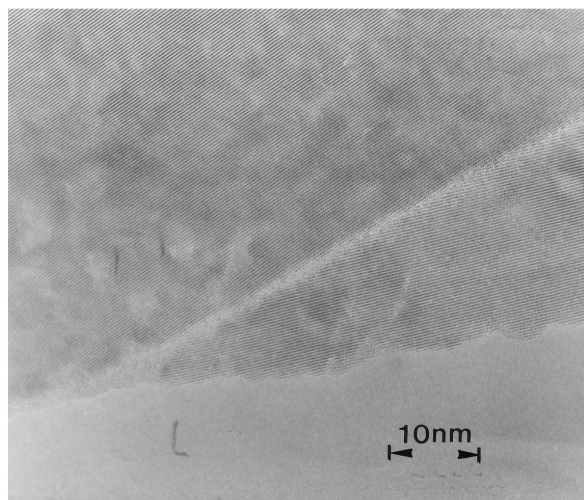
Oxide	Surface area (m^2/g)	Mean particle size (μm)	Purity
SnO_2^{a}	9.2	0.09	> 99.9
CoO^{b}	3.6	0.29	> 99.0

^a E. Merck, Darmstadt, Germany.

^b Aldrich Chemical Co., Milwaukee, WI.



(a)



(b)

Fig. 2. High resolution TEM micrograph of 0.5 mol% CoO doped SnO_2 sintered during 1 h at: (a) 1210°C; and (b) 1400°C.

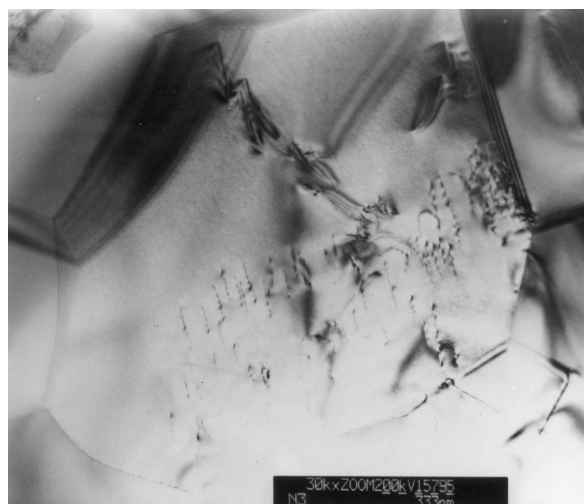


Fig. 3. TEM micrograph of 0.5 mol% CoO doped SnO_2 sintered at 1210°C during 1 h.

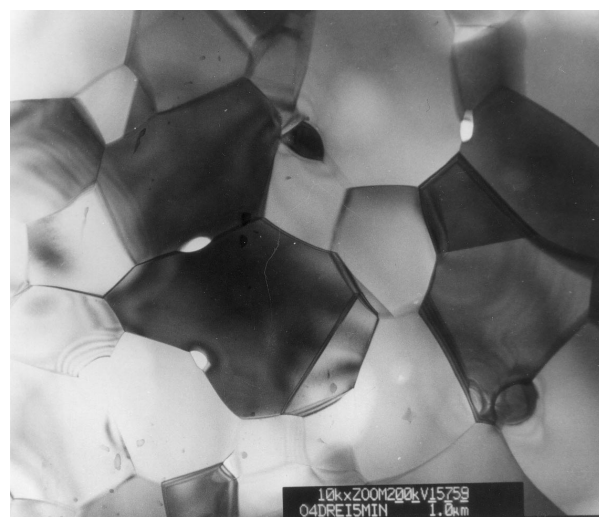


Fig. 4. TEM micrograph of 0.5 mol% CoO doped SnO_2 sintered at 1400°C during 1 h.

absent when the ceramic is sintered at 1400°C, where because of the low stability of these defects they diffuse to the grain boundary forming the amorphous phase and precipitating into the new phase as observed in Fig. 4. This new phase shown in Fig. 4 precipitated adjacent to the triple point was analysed by EDS revealing the presence of Sn and Co atoms. Compositional analysis based on EDS data yielded an approximate atomic ratio of 2 to 1 for Co and Sn atoms present in the phase. Convergent beam electron diffraction (CBED) patterns taken along various crystallographic orientations of the phase indicated a cubic point group, $m\bar{3}m$ for the crystal. The dimension of the unit cell was estimated from careful measurements of the diameter of the ring defined by the first order Laue zone present in the CBED patterns, and for this phase a cell parameter $a = 8.70(2) \text{ \AA}$ was determined from the $\langle 001 \rangle$, $\langle 110 \rangle$ and $\langle 111 \rangle$ zone axis patterns. In this context a convergent beam microdiffraction pattern exhibiting diffraction spots belonging to zero and first order Laue zones and taken along $[001]$ zone axis of the phase is shown in Fig. 5. Analysis of this pattern involving projection of the diffraction spots of the first order Laue zone on the zero order Laue zone yielded a $\langle 001 \rangle$ projected pattern of a body centered cubic cell. This clearly indicates that the reciprocal lattice of the phases is body-centered and that the Bravais lattice is in consequence face-centered. Extinction conditions of diffraction derived from the superimposed pattern indicate diamond glide along $\langle 111 \rangle$ of the unit cell. Introduction of this diamond glide into the $m\bar{3}m$ point group of the face-centered cubic cell suggests the space group of the phase to be $Fd\bar{3}m$. The chemical and crystal data thus determined upon comparison with those reported [9] for crystalline materials unambiguously establish the identity of the phase as Co_2SnO_4 .

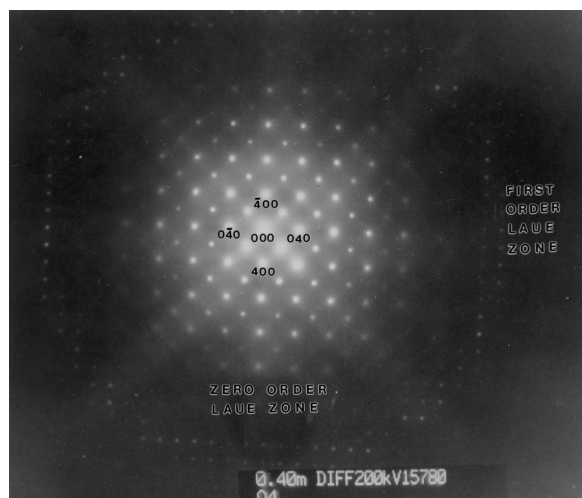


Fig. 5. Electron diffraction pattern for the precipitated phase adjacent to the triple point of the 0.5 mol% CoO doped SnO_2 microstructure.

The observations of the TEM micrographs confirm that no liquid is formed during sintering and suggest that the new phase is formed by diffusion of Co related defects to the grain boundary creating instability for solid state precipitation. The results of this study are consistent with the observations by Cerri et al. [9] that the densification of CoO doped SnO_2 is promoted by enhanced solid state diffusion from oxygen vacancy creation near to the grain boundaries of the SnO_2 grains. They also reported as identified by X-ray diffraction the precipitation of Co_2SnO_4 phase after sintering of 8 mol% CoO doped SnO_2 . However, this phase was not observed by high temperature X-ray diffraction up to 1150°C indicating that this phase is precipitated during cooling. Because of the X-ray diffraction detection limit the Co_2SnO_4 phase was not observed after sintering of 2 mol% CoO doped SnO_2 in their study.

4. Conclusions

High resolution TEM micrographs showed that an amorphous-like phase, probably with a high oxygen vacancy content and low in cobalt is formed near

the grain boundaries of 0.5 mol% CoO doped SnO_2 sintered to >99%. TEM microscopy also revealed the solid state precipitation of a secondary phase near the triple points in the grain boundary regions identified by EDS and by electron diffraction to be Co_2SnO_4 .

Acknowledgements

The authors acknowledge Conselho Nacional de Desenvolvimento Científico e Tecnológico (CNPq), Fundação ao Amparo à Pesquisa do Estado de São Paulo (FAPESP) and Financiadora de Estudos e Projetos (FINEP), all Brazilian Research Agencies for the financial support of this work.

References

- [1] J.G. Fagan, V.R.W. Amarakoon, Reliability and reproducibility of ceramic sensors: Part III, Humidity sensors, *Am. Ceram. Soc. Bull.* 72 (3) (1993) 119–130.
- [2] P. Olivi, E.C.P. Souza, E. Longo, J.A. Varela, L.O.S. Bulhões, Preparation and characterization of a dip-coated SnO_2 film for transparent electrodes for transmissive electrochromic devices, *J. Electrochem. Soc.* 140 (1993) L81.
- [3] V.G. Panteleev, K.S. Ramm, T.I. Pronk'kina, *Glass and Ceramics* 46 (1990) 199.
- [4] H.D. Joss, Initial stage sintering of tin oxide, M. Sc. Thesis, University of Washington, Seattle, WA, 1975.
- [5] P.H. Duvigneaud, D. Reighard, Activated sintering of tin oxide, in: P. Vicenzini (Ed.), *Science of Sintering*, vol. 12, Ceramurgia Srl., Faenza, Italy, 1980, pp. 287–292.
- [6] J.A. Varela, O.J. Whittemore, M.J. Ball, Structural evolution during the sintering of SnO_2 and SnO_2 –2 mole% CuO, in: G. C. Kuczynski, D.P. Uskokovic, H. Palmour, III, M.M. Ristic (Eds.), *Sintering '85*, Plenum Press, New York, 1987, pp. 259–268.
- [7] S. Zuca, M. Terzi, M. Zaharescu, K. Matiasovsky, Contribution to the study of SnO_2 -based ceramics: Part II. Effect of various oxide additives on the sintering capacity and electrical conductivity of SnO_2 , *J. Mater. Sci.* 26 (1991) 1673–1676.
- [8] S.J. Park, K. Hirota, H. Yamamura, Densification of nonadditive SnO_2 by hot isostatic pressing, *Ceram. Int.* 10 (3) (1984) 115–116.
- [9] J.A. Cerri, E.R. Leite, D. Gouvea, E. Longo, J.A. Varela, Effect of cobalt (II) oxide and manganese (IV) oxide on sintering of tin (IV) oxide, *J. Am. Ceram. Soc.* 79 (3) (1996) 799–804.
- [10] D. Gouvea, J.A. Varela, A. Smith, J.P. Bonnet, Morphological characteristics of SnO_2 based powders containing manganese, *Eur. J. Solid State Inorg. Chem.* 33 (1996) 343–354.
- [11] JCPDS File, Intern. Ctr. for Diffraction, 12 Campus Blvd, Newtown Square, PA, USA, 1993.